Preprints (www.preprints.org) | NOT PEER-REVIEWED | Posted: 18 April 2022 doi:10.20944/preprints202204.0159.v1

A modified piecewise relaxation method for singular initial value problems

Olumuyiwa Otegbeye [*1], **Shina D. Oloniiju** [†2], **and Gerald Marewo** [‡3]

[1]School of Computer Science and Applied Mathematics, University of Witwatersrand, Private Bag 3, Johannesburg 2050, South Africa.
[2]Department of Mathematics, Rhodes University, Makhanda, PO Box 94, Grahamstown 6140, South Africa.
[3]Department of Mathematics and Applied Mathematics, North West University, Private Bag X6001, Potchefstroom 2520, South Africa.

ABSTRACT

In gravitational theory and astrophysical dynamics, singular initial value problems (IVPs) are frequently encountered. Finding the solutions to this class of IVPs can be challenging due to their complex nature. This study strives to circumvent the complexity by proposing a numerical method for solving such problems. The approach proposed in the current research seeks solutions to the IVP by partitioning the domain $[0,L]$ of the problem into two intervals and solving the problem on each domain. The study seeks a closed-form solution to the IVP in the interval containing the singular point. A linearization technique and piecewise partitioning of the domain not containing the singularity are applied to the nonlinear IVP. The resulting linearized differential equation is solved using the Chebyshev spectral collocation method. Some examples are presented to illustrate the efficiency of the proposed method. Numerical analysis of the solution and residual errors are shown to ascertain convergence and accuracy. The results suggest that the technique gives accurate convergent solutions using a few collocation points.

keywords: relaxation, spectral methods, multi-domain.

1 Introduction

This study considers a class of singular second-order initial value problems (IVPs) of the form

$$y'' + \frac{\gamma}{x}y' + f(x,y) = 0, \qquad 0 < x \leq L, \tag{1}$$

with initial conditions

$$y(0) = y_0, \qquad y'(0) = y'_0, \tag{2}$$

where $f(x,y)$ is a nonlinear function and $\gamma > 0$. This class of initial value ordinary differential equation is ubiquitous in various models of mathematical physics and astrodynamics [1–3]. It is a regular occurrence in fields such as the theory of density distribution of isothermal gas sphere, the study of the gravitational potential of a completely degenerate white dwarf star, the theory of thermionic currents, and the analysis of self-gravitating spheres of plasma. The Lane-Emden, the Emden-Chandrasekhar, the Emden-Fowler and the Chandrasekhar's white dwarf equations are examples of this class of initial value problem.

Extensive research has been carried out to introduce new analytical, approximate and numerical methods for solving this class of IVPs. Wazwaz [4] used the variation iteration method to solve a class of singular Emden–Fowler equations. The variation iteration method (VIM) can be quite slow, long and even difficult to integrate beyond certain iterations, yet, it is easy to overcome the singularity at $x = 0$. The method presented in Turkyilmazoglu [5] is based on using the linear combinations of well-chosen basis functions such as the power function to approximate the solution. The expansion coefficients are then determined using a tau–like procedure. Liao [6] used the homotopy analysis method to obtain the solutions of selected singular IVPs. However, this method requires using an optimization parameter to control the convergence of the solution. This means that convergence cannot be guaranteed without a properly chosen control parameter. Other methods that have been studied

*Corresponding author. olumuyiwa.otegbeye@wits.ac.za
†s.oloniiju@ru.ac.za
‡gerald.marewo@nwu.ac.za

Preprints (www.preprints.org) | NOT PEER-REVIEWED | Posted: 18 April 2022 doi:10.20944/preprints202204.0159.v1

include the finite difference method [7, 8], the Adomian decomposition method [9], the homotopy perturbation method [10] and many more [11, 12].
One main difficulty in obtaining numerical solutions to this class of IVPs is the singularity at the origin. To circumvent this singularity, Marewo [13] proposed a modified spectral relaxation method that introduces a tolerance point not far from the singular point, thus splitting the domain into two sub-domains. This study aims to propose a technique that circumvents the singularity at $x = 0$ as presented in [13], and further solves the IVP using a piecewise pseudospectral relaxation method in each sub-interval [14, 15]. Some selected singular IVPs were solved to demonstrate the effectiveness of the proposed approach.

2 Description of the Method

This section describes the proposed method, which will be referred to as the modified piecewise relaxation method (MPRM). The MPRM involves splitting the domain $[0,L]$ into $[0,\varepsilon]\cup[\varepsilon,L]$, where ε is chosen to be a small perturbation away from the point of singularity. The linearization technique studied in Ramos [16] is applied on the domain $[0,\varepsilon]$, the piecewise spectral relaxation method is used on $[\varepsilon,L]$. Suppose that the nonlinear IVP in Equations (1) and (2) is expressed in the form

$$y'' = f(x,y,y'), \qquad y(0) = y_0, \quad y'(0) = y_0', \tag{3}$$

where $f(x,y,y')$ is a nonlinear function of x,y,y' which contains a singularity at $x = 0$. Assume $f(x,y,y')$ is a regular function, then it can be approximated using the Taylor series expansion about the point (ε,y_0,y_0'), such that Equation (3) is expressed as

$$y'' - G_0y' - H_0y = Q_0(x,\varepsilon,y_0,y_0'), \tag{4}$$

where

$$Q_0(x,\varepsilon,y_0,y_0') = F_0 + J_0(x-\varepsilon) - H_0y_0 - G_0y_0', \tag{5}$$

and

$$F_0 = f(\varepsilon,y_0,y_0'), \quad J_0 = \frac{\partial f}{\partial x}(\varepsilon,y_0,y_0'), \quad H_0 = \frac{\partial f}{\partial y}(\varepsilon,y_0,y_0'), \quad G_0 = \frac{\partial f}{\partial y'}(\varepsilon,y_0,y_0'). \tag{6}$$

Equation (4) is a nonhomogeneous linear ordinary differential equation whose solution can be found by the usual method of finding the complementary function and particular integral of the equation. Thus, the analytical solution to eq. (4) is obtained as

$$y(x) = A_0\exp(\kappa_+(x-\varepsilon)) + B_0\exp(\kappa_-(x-\varepsilon)) + C_0(x-\varepsilon) + D_0, \tag{7}$$

where

$$\kappa_\pm = \frac{G_0 \pm \sqrt{G_0^2+4H_0}}{2}, \quad C_0 = -\frac{J_0}{H_0}, \quad D_0 = -\frac{(G_0C_0 + F_0 - H_0y_0 - G_0y_0')}{H_0}. \tag{8}$$

It should be noted here that a real-valued solution to Equation (4) does not exist if $G_0^2+4H_0 < 0$. The constants A_0 and B_0 are obtained by using the initial conditions at $x = 0$ so that we have

$$A_0 = \left((y_0' - C_0) - \kappa_-(y_0 + C_0\varepsilon - D_0)\right)\frac{e^{\kappa_+\varepsilon}}{(\kappa_+ - \kappa_-)}, \tag{9}$$

$$B_0 = \left(-(y_0' - C_0) + \kappa_+(y_0 + C_0\varepsilon - D_0)\right)\frac{e^{\kappa_-\varepsilon}}{(\kappa_+ - \kappa_-)}. \tag{10}$$

Therefore, the values of the constants A_0, B_0, C_0, D_0 can be used to obtain the initial conditions

Preprints (www.preprints.org) | NOT PEER-REVIEWED | Posted: 18 April 2022 doi:10.20944/preprints202204.0159.v1

$$y(\varepsilon) = A_0 + B_0 + D_0 \tag{11}$$
$$y'(\varepsilon) = \kappa_+ A_0 + \kappa_- B_0 + C_0, \tag{12}$$

which will then be used to solve the IVP in the domain $[\varepsilon, L]$. Upon obtaining the solution $y(x)$ in the interval $[0, \varepsilon]$, the following non-singular IVP

$$y'' + \frac{\gamma}{x} y' + f(x,y) = 0, \quad \varepsilon \le x \le L$$
$$y(\varepsilon) = y_\varepsilon, \qquad y'(\varepsilon) = y'_\varepsilon \tag{13}$$

is solved by decomposing the domain $[\varepsilon, L]$ into equal subintervals and approximating $y(x)$ and its derivative in terms of the Lagrange polynomials as basis functions. y_ε and y'_ε are approximately obtained using Equations (11) and (12) respectively. First, Equation (13) is disintegrated into a system of two first-order initial value problems as

$$y'(x) = z(x), \qquad y(\varepsilon) = y_\varepsilon \tag{14}$$
$$z'(x) + \frac{\gamma}{x} z(x) = -f(x,y), \qquad z(\varepsilon) = y'(\varepsilon) = y'_\varepsilon. \tag{15}$$

Next, the domain $[\varepsilon, l]$ is decomposed into equal non–overlapping intervals $\Gamma_i = \{[x^{i-1}, x^i] : i = 1, 2, \ldots, P\}$, such that $x^0 = \varepsilon$ and $x^P = L$. Let $\{y^1(x),\, z^1(x)\}$ be the solution in the first subinterval $[\varepsilon, x^1]$, we use the continuity condition to determine the initial condition for solving the IVP consisting of eqs. (14) and (15) in subsequent subintervals. Therefore, in each subinterval $[x^{i-1}, x^i]$, the iterative scheme

$$\frac{d}{dx} y^i_{r+1}(x) = z^i_r(x) \tag{16}$$
$$\frac{d}{dx} z^i_{r+1}(x) + \frac{\gamma}{x} z^i_{r+1} = -f^i_r(x, y^i_r), \tag{17}$$

is solved subject to

$$y^{i-1}_{r+1}(x^{i-1}) = y^i_{r+1}(x^{i-1}) \tag{18}$$
$$z^{i-1}_{r+1}(x^{i-1}) = z^i_{r+1}(x^{i-1}). \tag{19}$$

The proposed iterative scheme follows the Gauss-Seidel approach of linearizing algebraic equations by decoupling the system. The above system of decoupled equations can be solved using any known analytical or numerical methods. However, we will employ the spectral collocation method to solve the system in each subinterval. The spectral method is premised on approximating the solution as a truncated linear combination of certain basis functions. In this study, the Lagrange interpolating polynomials are used as basis functions, and the solutions are evaluated on the Chebyshev-Gauss-Lobatto nodes $\tilde{x} \in [-1, 1]$ defined as

$$\tilde{x} = -\cos\left(\frac{j\pi}{N}\right), \quad j = 0, 1, 2, \ldots, N. \tag{20}$$

Each subinterval $[x^{i-1}, x^i]$ is transformed to $[-1, 1]$ using the affine mapping

$$x = \frac{x^i - x^{i-1}}{2}\tilde{x} + \frac{x^i + x^{i-1}}{2}. \tag{21}$$

The functions and their first order derivatives are approximated as

$$\left\{\frac{d}{dx}y^i_{r+1}(x),\ \frac{d}{dx}z^i_{r+1}(x)\right\}=\left\{\sum_{k=0}^{N}\mathbf{D}_{jk}y^i_{r+1}(x^i_k),\ \sum_{k=0}^{N}\mathbf{D}_{jk}y^i_{r+1}(x^i_k)\right\}=\left\{\mathbf{DY}^i_{r+1},\ \mathbf{DZ}^i_{r+1}\right\},\ j=0,1,\ldots,N, \tag{22}$$

where $\mathbf{D}=2D/(x^i-x^{i-1})$, D is the Chebyshev differentiation matrix defined in Trefethen [17], while $\mathbf{Y}^i_{r+1}=[y^i_{r+1}(x^i_0),\ldots,y^i_{r+1}(x^i_N)]$ and $\mathbf{Z}^i_{r+1}=[z^i_{r+1}(x^i_0),\ldots,z^i_{r+1}(x^i_N)]$ are respectively vector functions of the solutions $y(x)$ and $z(x)$ at the collocation points x^i_j. Applying spectral collocation on Equations (16) and (17) results in

$$[\mathbf{D}]\mathbf{Y}^i_{r+1}=\mathbf{Z}^i_r \tag{23}$$

$$\left[\mathbf{D}+\mathrm{diag}(\gamma/x^i)\right]\mathbf{Z}^i_{r+1}=-\mathbf{F}^i_r, \tag{24}$$

with initial conditions

$$\mathbf{Y}^i_{r+1}(x_0)=\mathbf{Y}^{i-1}_{r+1}(x_N),\quad \mathbf{Z}^i_{r+1}(x_0)=\mathbf{Z}^{i-1}_{r+1}(x_N),\quad \mathbf{Y}^1_{r+1}(x_0)=y_\varepsilon,\quad \mathbf{Z}^1_{r+1}(x_0)=y'_\varepsilon, \tag{25}$$

where $\mathbf{F}^i_r=[f^i_r(x_0,y^i(x_0)),\ldots,f^i_r(x_N,y^i(x_N))]$.

3 Illustrative Examples

The technique proposed above is demonstrated using selected singular IVPs, such as the nonlinear homogeneous and nonhomogeneous Lane-Emden and the Emden-Fowler equations.

Example 3.1 (Nonlinear homogeneous Lane-Emden equation)**.**

$$y''+\frac{2}{x}y'+y^n=0,\quad y(0)=1,\ y'(0)=0, \tag{26}$$

where n is the polytropic index defined in the range $0\le n\le 5$. Analytical solutions have been studied for $n=1,5$ and are given respectively as [18, 19]

$$y(x)=\frac{\sin x}{x},\quad y(x)=\frac{1}{\sqrt{1+\frac{x^2}{3}}}. \tag{27}$$

Example 3.2 (Nonlinear homogeneous Emden-Fowler equation)**.**

$$y''+\frac{1}{x}y'-y^3+3y^5=0,\quad y(0)=1,\ y'(0)=0, \tag{28}$$

whose exact solution was given in Wazwaz [4] as $y(x)=\dfrac{1}{\sqrt{1+x^2}}$.

Example 3.3 (Nonlinear homogeneous Emden-Fowler equation)**.**

$$y''+\frac{6}{x}y'+14y+4y\ln y=0,\quad y(0)=1,\ y'(0)=0, \tag{29}$$

and the analytical solution is given as $y(x)=e^{-x^2}$ *[20].*

4 Results and discussion

This section discusses some results obtained when the technique proposed in this study is applied to examples (3.1)−(3.3). These examples have closed-form solutions, and the numerical approximations obtained herein are compared with these closed-form solutions. The absolute errors obtained by taking the difference between the numerical solutions and the exact solutions at selected collocation points are presented. The solution and residual errors analyses are conducted for convergence and accuracy.

Table 1 shows the numerical and exact solutions of Example 3.1.

Preprints (www.preprints.org) | NOT PEER-REVIEWED | Posted: 18 April 2022 doi:10.20944/preprints202204.0159.v1

Table 1. Example 3.1: Comparison of the numerical solutions $y_N(x)$ obtained using the proposed method with the exact solutions $y(x)$ for $n=1$, $n=5$, taking $\varepsilon = 1\times10^{-10}$, $N=10$ and $P=20$.

	$n=1$		$n=5$	
x	$y_N(x)$	$y(x)$	$y_N(x)$	$y(x)$
ε	1.00000	1.00000	1.00000	1.00000
1	0.84147	0.84147	0.86601	0.86601
2	0.45465	0.45465	0.65465	0.65465
3	0.04704	0.04704	0.50000	0.50000
4	−0.18920	−0.18920	0.39736	0.39736
5	−0.19179	−0.19179	0.32733	0.32733
6	−0.04657	−0.04657	0.27735	0.27735
7	0.09386	0.09386	0.24019	0.24019
8	0.12367	0.12367	0.21160	0.21160
9	0.04579	0.04579	0.18898	0.18898
10	−0.05440	−0.05440	0.17066	0.17066

From Table 1, it can be seen that the numerical solutions are in excellent agreement with the analytical solutions up to 5 decimal places. This trend is observed at all the grid points in the domain $[\varepsilon, L]$ for $n=1$ and 5. This result shows that the MPRM is capable of solving such problems. The results were generated using ten collocation points, suggesting that very few points can obtain highly accurate approximate solutions. To investigate the difference between the exact and approximate solutions, the absolute error is presented in Table 2, and we show the errors at selected points ε, x_1 and x_L from the interval $[x_0=\varepsilon, x_L=L]$. The point x_0 is of particular interest here because regardless of the number of subintervals used, the error at x_0 remains the same. Hence, there will be consistency in comparing the absolute error at this point.

Table 2. Example 3.1: Effect of increasing the number of sub-intervals on the absolute error $\max_{0\le j\le N}|y_N(x_j)-y(x_j)|$ taking $\varepsilon = 1\times10^{-10}, L=10$ and $N=10$.

	$n=1$ $\max_{0\le j\le N}\lvert y_N(x_j)-y(x_j)\rvert$					
x	$P=10$	$P=20$	$P=30$	$P=40$	$P=50$	$P=100$
ε	1.17×10^{-21}	1.17×10^{-21}	1.17×10^{-21}	1.17×10^{-21}	1.17×10^{-21}	1.17×10^{-21}
x_1	3.25×10^{-14}	1.62×10^{-14}	1.08×10^{-14}	8.12×10^{-15}	6.49×10^{-15}	3.25×10^{-15}
x_L	1.29×10^{-15}	6.44×10^{-16}	4.29×10^{-16}	3.22×10^{-16}	2.58×10^{-16}	1.29×10^{-16}
	$n=5$ $\max_{0\le j\le N}\lvert y_N(x_j)-y(x_j)\rvert$					
x	$P=10$	$P=20$	$P=30$	$P=40$	$P=50$	$P=100$
ε	1.17×10^{-21}	1.17×10^{-21}	1.17×10^{-21}	1.17×10^{-21}	1.17×10^{-21}	1.17×10^{-21}
x_1	3.24×10^{-14}	1.62×10^{-14}	1.08×10^{-14}	8.12×10^{-15}	6.49×10^{-15}	3.25×10^{-15}
x_L	3.79×10^{-15}	1.9×10^{-15}	1.26×10^{-15}	9.51×10^{-16}	7.61×10^{-16}	3.81×10^{-16}

From Table 2, it is observed that at $x=\varepsilon$, the absolute error is the smallest. This small error is due to the small magnitude of the chosen value of ε. This result indicates that the aim of the MPRM in avoiding the singularity by perturbing the initial position will not have a significant impact on the accuracy of the approximate solutions obtained for $x\in[\varepsilon, L]$. The result also shows that 20 and 40 subintervals are sufficient to produce the smallest absolute errors for $n=1$ and $n=5$, respectively. This trend suggests that the more nonlinear a given problem is, the higher the number of subintervals needed. It can also be observed from Table 2 that using a lot of subintervals is not necessary because the effect on the absolute error is negligible. To illustrate Table 2 graphically, Figure 1 portrays the absolute error of Example 3.1 as the interval increases (using a step-size of 1) when 20 sub-intervals are used for the case $n=5$.

Preprints (www.preprints.org) | NOT PEER-REVIEWED | Posted: 18 April 2022 doi:10.20944/preprints202204.0159.v1

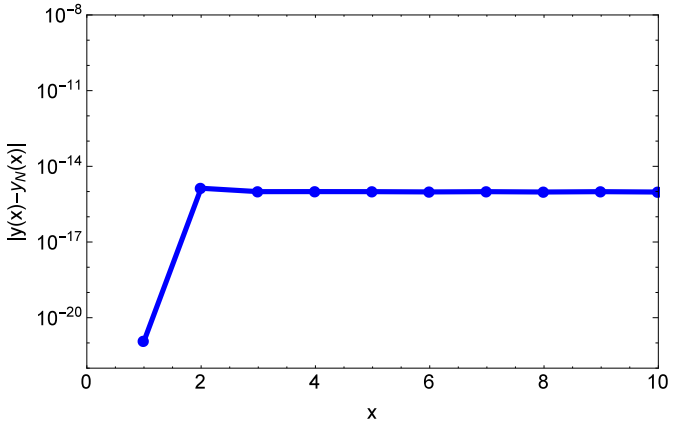

Figure 1. Example 3.1: Absolute error defined as $|y(x) - y_N(x)|$ when $n = 5$, $P = 20$ and $N = 10$.

Figure 1 supports the results given in Table 2 where we observe that the absolute error is consistently 10^{-15} as x increases. Figure 2a and Figure 2b, respectively, show the numerical solutions $y_N(x)$ and $y'_N(x)$ of the homogeneous Lane-Emden equations for the cases $n = 1$ and $n = 5$. Figure 2a and Figure 2b show variations in the solutions $y_N(x)$ and $y'_N(x)$, where overlap in solutions when $n = 1$ and distinct solutions when $n = 5$ are observed.

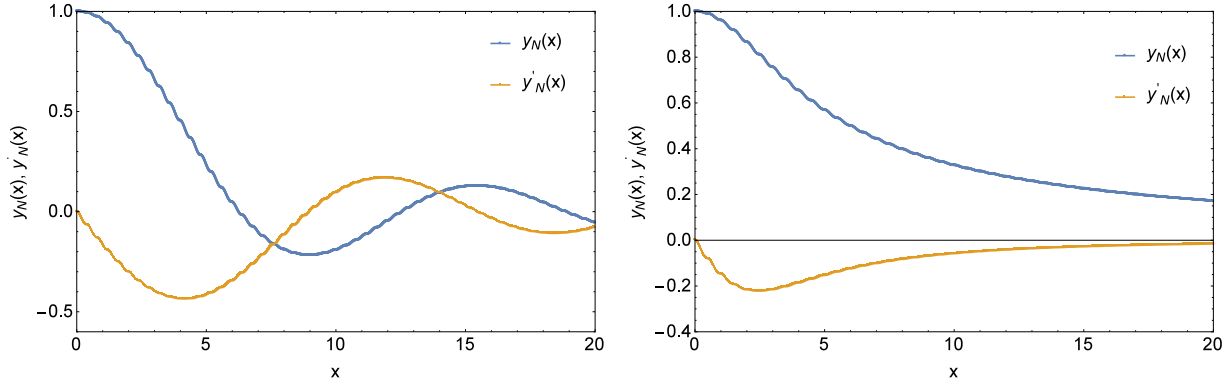

(a) $n = 1$ **(b)** $n = 5$

Figure 2. Example 3.1: Numerical solutions $y_N(x)$ and $y'_N(x)$ for (a) $n = 1$, (b) $n = 5$ using $P = 20$ and $N = 10$.

The solution and residual errors are calculated to verify the convergence and accuracy of these approximate solutions. The solution error is obtained by taking the infinity norm of the difference between approximate solutions obtained after each successive iteration.

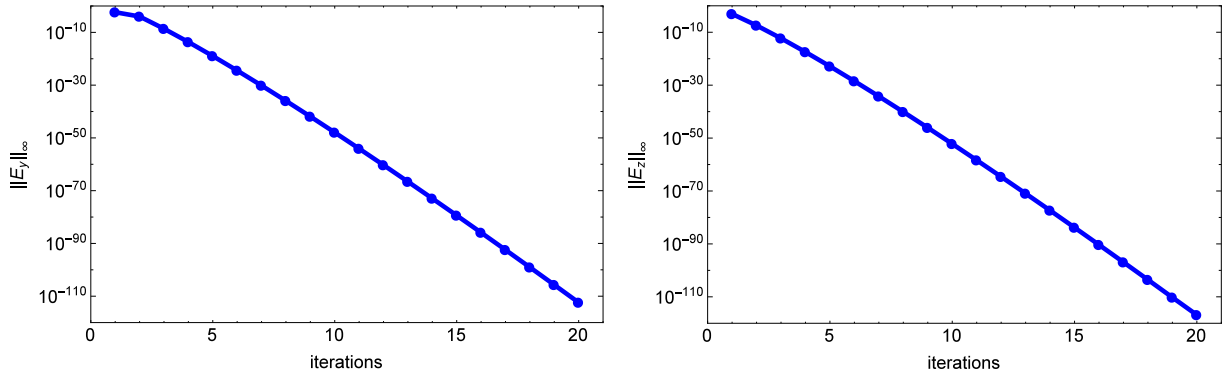

(a) Solution error for $y(x)$ **(b)** Solution error for $y'(x)$

Figure 3. Example 3.1: Solution errors for $y_N(x)$ and $y'_N(x)$ for $n = 5$ using $P = 20$ and $N = 20$.

Preprints (www.preprints.org) | NOT PEER-REVIEWED | Posted: 18 April 2022 doi:10.20944/preprints202204.0159.v1

Figure 3 shows the graph of the infinity norm of the solution errors for $y_N(x)$ and $y'_N(x)$ against iterations. It can be seen from the figure that as iterations increase, the convergence of the numerical solution improves because the error between successive iterations becomes smaller. It is observed that at the $20th$ iteration, the error is 10^{-110}, which is quite small. Even though total convergence to a consistent error is not attained, a further decrease in error is negligible, thus rendering the solutions obtained using the MPRM convergent to minimal tolerance levels. The slope of the graph shows that the solutions converge linearly due to the decoupling of the original equation. If tolerance of 10^{-10} is selected, it can be observed that it will take 5 iterations to reach convergence.

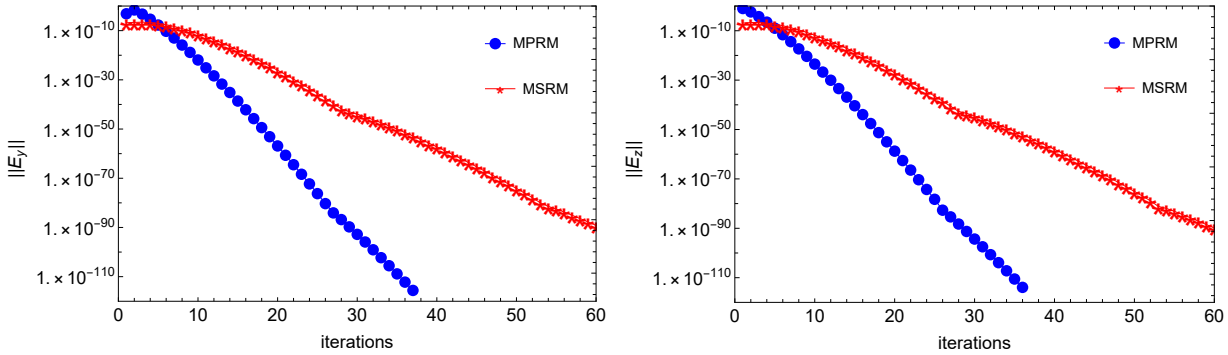

(a) Solution error for $y(x)$ using the MPRM and MSRM **(b)** Solution error for $y'(x)$ using the MPRM and MSRM

Figure 4. Example 3.1: Comparing solution errors for $y_N(x)$ and $y'_N(x)$ for $n = 5$ using $P = 10$ and $N = 30$.

A comparison is performed on the speed of convergence of solutions to Example 3.1 to show that MPRM improves the convergence speed of MSRM. It is observed from Figure 4 that the MPRM converges faster than MSRM. We also note that the MPRM converges to a smaller error $\left(10^{-120}\right)$ with less than 40 iterations while the MSRM has a bigger error after 60 iterations $\left(10^{-90}\right)$. The results indicate that the MPRM improved the convergence speed of the MSRM, which is remarkable given that the MSRM shows an impressive speed of convergence and a small error after a few iterations.

The residual error is used to test for accuracy. The residual error is obtained by substituting the approximate solutions into Example 3.1 and calculating the infinity norm. Figure 5 shows the residual error at different iteration levels. From Figure 5, it is observed that the residual error norm is at 10^{-114} at all the iteration points. This result shows that the solutions obtained using the MPRM for this problem are accurate.

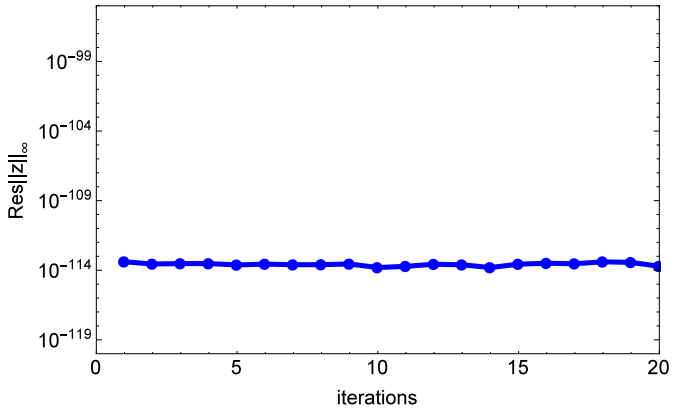

Figure 5. Example 3.1: Residual error when $n = 5$ using $P = 20$ and $N = 20$.

Figure 6 portrays the absolute difference between the exact and numerical solutions of Example 3.2. It is observed from Figure 6 that the absolute error between the different solutions is small, as it can be seen to be about 10^{-13} on average. This result indicates that the MPRM gives an accurate solution. Figure 7 shows the solution error norms of $y_N(x)$ and $y'_N(x)$ as the number of iterations increases. From Figure 7, it can be seen that the MPRM converges more or less linearly and to a small error. It is noted here that although full convergence is not obtained at the $20th$ iteration, the solution error at that point is 10^{-80}. This convergence result implies that setting a tolerance level less than 10^{-80} can lead to absolute convergence of the solutions.

Preprints (www.preprints.org) | NOT PEER-REVIEWED | Posted: 18 April 2022 doi:10.20944/preprints202204.0159.v1

In Figure 7, the residual error norm of Example 3.2 is shown as iteration is increased. It can be seen from Figure 7 that as the number of iterations increases, the residual error of Example 3.2 is noted to be significantly small, with a small difference at each iteration.

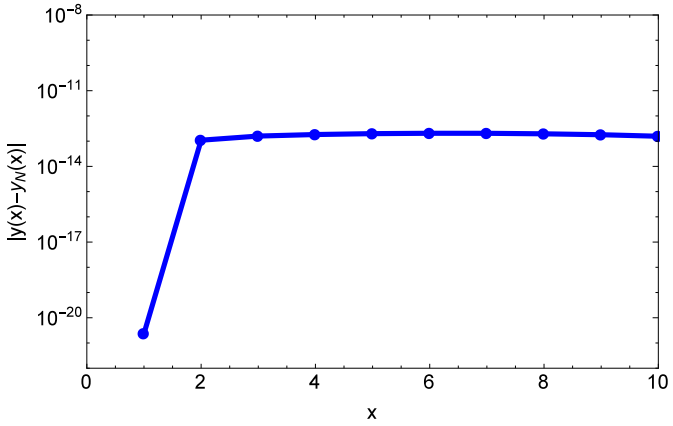

Figure 6. Example 3.2: Absolute error defined as $|y(x) - y_N(x)|$ when $P = 20$ and $N = 10$.

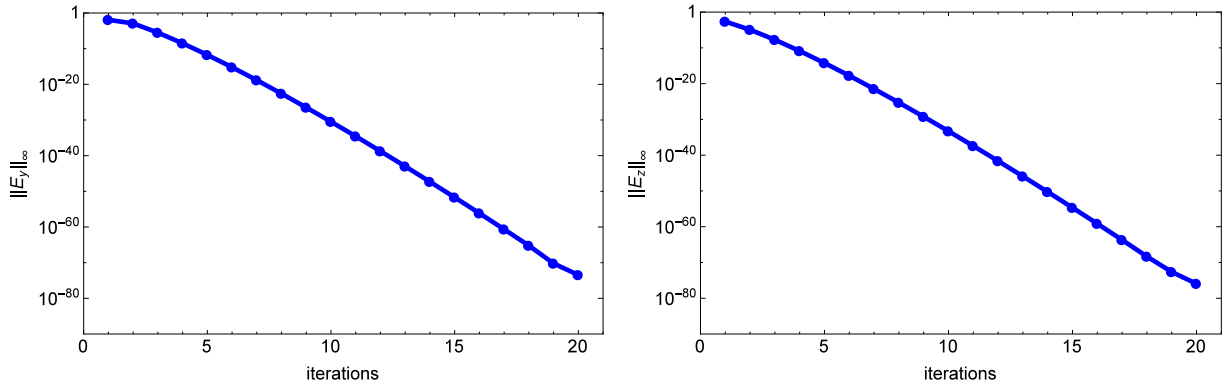

Figure 7. Example 3.2: Solution errors for $y_N(x)$ and $y'_N(x)$ when $P = 20$ and $N = 20$.

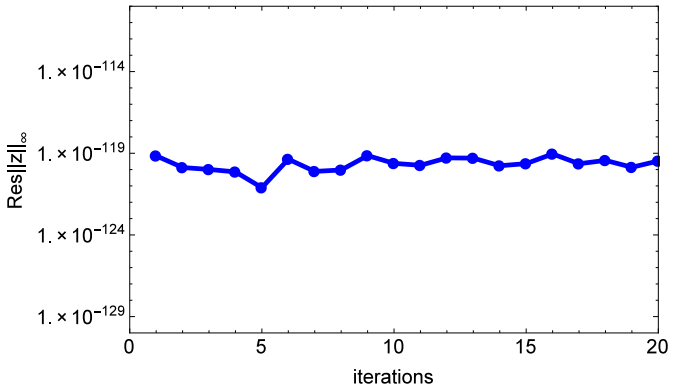

Figure 8. Example 3.2: Residual error for equation Example 3.1 when $P = 20$ and $N = 20$.

In Figure 9, the absolute error between the exact and numerical solution of Example 3.3 is presented. It is observed from Figure 9 that the absolute error is minimal, and the maximum error is approximately 10^{-14}. Similar results are shown in Figure 1 and Figure 6. We present the absolute error as the number of subintervals is increased in Figure 10. It can be seen that as the number of subintervals increases, the absolute error decreases. The result also shows that when the subintervals are

Preprints (www.preprints.org) | NOT PEER-REVIEWED | Posted: 18 April 2022 doi:10.20944/preprints202204.0159.v1

increased beyond 40, there is no significant effect on the absolute maximum error. This result implies that for this problem and similar problems, 40 subintervals are enough to produce the smallest error between actual and approximate solutions. The solution error norms of $y_N(x)$ and $y'_N(x)$ are presented in Figure 11. From Figure 11, as the number of iterations increases, the solution error norm becomes smaller. At the $20th$ iteration, the solution error reduces linearly to 10^{-60}, which shows that the difference between subsequent solutions obtained using the MPRM is negligible. Figure 12 show that the residual error norm of Example 3.3 is minimal at 10^{-119} which indicates that the MPRM is an accurate method for such problems. In Table 3, we present a comparison between solutions obtained using the MPRM, Chebyshev neural networks, and artificial neural networks Mall and Chakraverty [20] against the exact solution to ascertain the accuracy of the method presented in this study. From Table 3, it is observed that at all the grid points in x, the MPRM gives the same solution as the exact up to 8 decimal places, thereby indicating that the MPRM gives better solutions to the IVP compared to the methods used by Mall and Chakraverty [20].

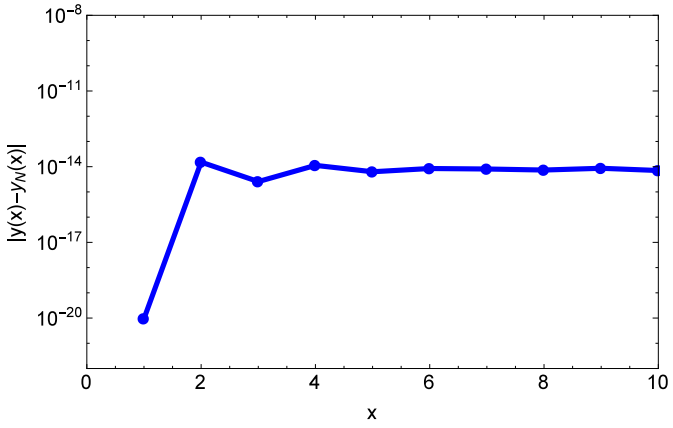

Figure 9. Example 3.3: Absolute error defined as $|y(x) - y_N(x)|$ when $P = 20$ and $N = 10$.

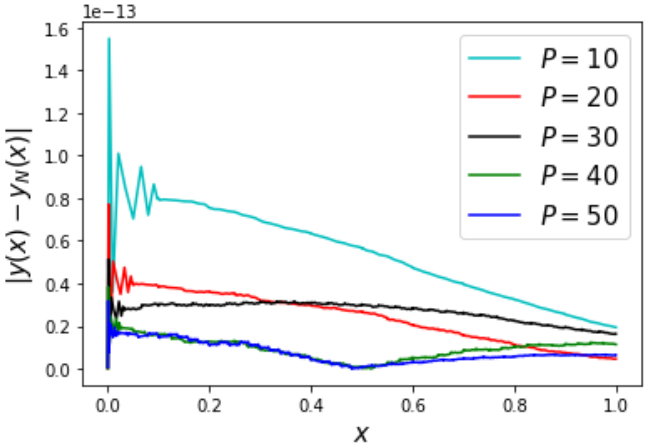

Figure 10. Example 3.3: Absolute error defined as $|y(x) - y_N(x)|$ plots different number of sub–intervals P and $N = 10$.

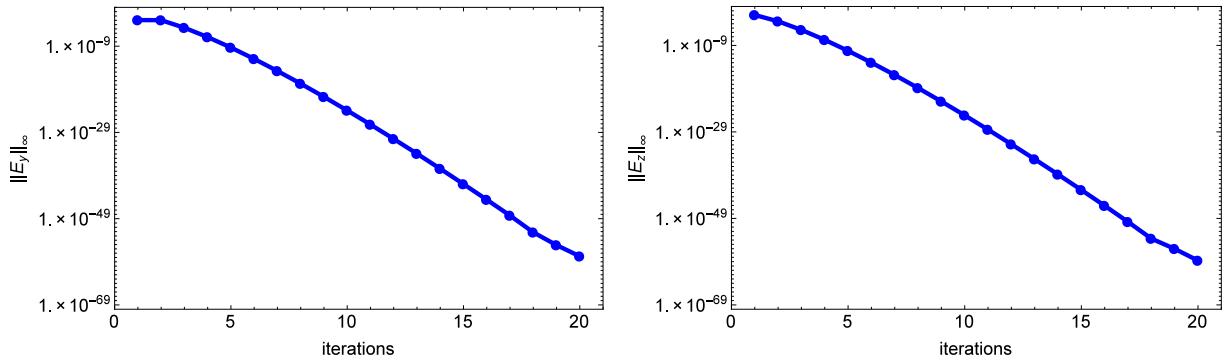

Figure 11. Example 3.3: Solution errors for $y_N(x)$ and $y'_N(x)$ when $P = 20$ and $N = 20$.

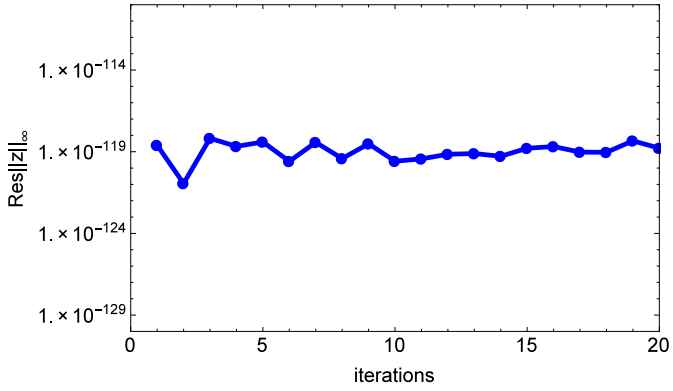

Figure 12. Example 3.3: Residual error for equation Example 3.1 when $P = 20$ and $N = 20$.

Table 3. Example 3.3: Comparison of the numerical solution obtained using the proposed method with the exact solution and the solutions presented in Mall and Chakraverty [20] using the Chebyshev neural network (ChNN) and the artificial neural network (ANN), with $N = 10$, $P = 10$, and $\varepsilon = 1 \times 10^{-10}$.

	Exact	Mall and Chakraverty [20]		Present study (MPRM)
x	$y(x)$	*ChNN*	*ANN*	$y_N(x)$
0.1	0.99004983	0.99004883	0.99014274	0.99004983
0.2	0.96078944	0.96077941	0.96021042	0.96078944
0.3	0.91393119	0.91393017	0.91302963	0.91393119
0.4	0.85214379	0.85224279	0.85376495	0.85214379
0.5	0.77880078	0.77870077	0.77644671	0.77880078
0.6	0.69767633	0.69767719	0.69755681	0.69767633
0.7	0.61262639	0.61272838	0.61264315	0.61262639
0.8	0.52729242	0.52729340	0.52752822	0.52729242
0.9	0.44485807	0.44490806	0.44502071	0.44485807
1.0	0.36787944	0.36782729	0.36747724	0.36787944

5 Conclusion

This study introduced and described the modified piecewise relaxation method (MPRM) and applied it to some singular initial value problems. The technique, which is premised on partitioning the domain $[0, L]$ into $[0, \varepsilon]$ and $[\varepsilon, L]$, bypassed the singularity at $x = 0$. Thus, making it easy to implement the piecewise spectral relaxation method. The results indicated that decomposing the interval $[\varepsilon, L]$ into non-overlapping subintervals improves the efficiency and accuracy of the approximate solution. The proposed MPRM was shown to be linearly convergent, requires few iterations to reach accuracy, easy to implement and gives

 doi:10.20944/preprints202204.0159.v1

better solutions compared to some methods in published literature. The proposed method requires few collocation points to produce accurate and convergent solutions. Finally, the MPRM does not require many subintervals to give good results.
In summary, the proposed modified piecewise relaxation method for solving singular initial value problems with one equation has been found to give convergent solutions that are highly accurate. The technique will be extended to systems of singular initial value problems and partial differential equations in future studies.

References

1. Subrahmanyan Chandrasekhar and Subrahmanyan Chandrasekhar. *An introduction to the study of stellar structure*, volume 2. Courier Corporation, 1957.
2. Harold Thayer Davis. *Introduction to nonlinear differential and integral equations*. US Atomic Energy Commission, 1960.
3. Owen Willans Richardson. *The emission of electricity from hot bodies*. Longmans, Green and Company, 1921.
4. Abdul-Majid Wazwaz. A reliable treatment of singular Emden–Fowler initial value problems and boundary value problems. *Applied Mathematics and Computation*, 217(24):10387–10395, 2011.
5. M Turkyilmazoglu. Effective computation of exact and analytic approximate solutions to singular nonlinear equations of Lane–Emden–Fowler type. *Applied Mathematical Modelling*, 37(14-15):7539–7548, 2013.
6. Shijun Liao. A new analytic algorithm of Lane–Emden type equations. *Applied Mathematics and Computation*, 142(1): 1–16, 2003.
7. RK Pandey. A finite difference method for a class of singular two point boundary value problems arising in physiology. *International journal of computer mathematics*, 65(1-2):131–140, 1997.
8. RK Pandey and Arvind K Singh. On the convergence of a finite difference method for a class of singular boundary value problems arising in physiology. *Journal of Computational and Applied Mathematics*, 166(2):553–564, 2004.
9. Abdul-Majid Wazwaz. Adomian decomposition method for a reliable treatment of the Emden–Fowler equation. *Applied Mathematics and Computation*, 161(2):543–560, 2005.
10. MSH Chowdhury and Ishak Hashim. Solutions of Emden–Fowler equations by homotopy-perturbation method. *Nonlinear Analysis: Real World Applications*, 10(1):104–115, 2009.
11. ASV Ravi Kanth and Vishnu Bhattacharya. Cubic spline for a class of non-linear singular boundary value problems arising in physiology. *Applied Mathematics and Computation*, 174(1):768–774, 2006.
12. M Abukhaled, SA Khuri, and A Sayfy. A numerical approach for solving a class of singular boundary value problems arising in physiology. *International Journal of Numerical Analysis and Modeling*, 8(2):353–363, 2011.
13. Gerald Tendayi Marewo. *A Modified Spectral Relaxation Method for some Emden-Fowler Equations*. intechOpen.
14. SS Motsa, P Dlamini, and M Khumalo. A new multistage spectral relaxation method for solving chaotic initial value systems. *Nonlinear Dynamics*, 72(1-2):265–283, 2013.
15. SS Motsa. A new spectral relaxation method for similarity variable nonlinear boundary layer flow systems. *Chemical Engineering Communications*, 201(2):241–256, 2014.
16. Juan I Ramos. Linearization techniques for singular initial-value problems of ordinary differential equations. *Applied Mathematics and Computation*, 161(2):525–542, 2005.
17. Lloyd N Trefethen. *Spectral methods in MATLAB*, volume 10. SIAM, 2000.
18. Shambhunath Srivastava. A new solution of the Lane-Emden equation of index n= 5. *The Astrophysical Journal*, 136: 680–681, 1962.
19. Hubert Goenner and Peter Havas. Exact solutions of the generalized Lane–Emden equation. *Journal of Mathematical Physics*, 41(10):7029–7042, 2000.
20. Susmita Mall and Snehashish Chakraverty. Numerical solution of nonlinear singular initial value problems of Emden–Fowler type using Chebyshev Neural Network method. *Neurocomputing*, 149:975–982, 2015.